2018

Deciphering the Rules of Cell-to-Cell Coupling by Molecular Modeling and Simulation

Linda D. Lee
Portland State University, ldlee3@alaska.edu

Deciphering the Rules of Cell-to-Cell Coupling by Molecular Modeling and Simulation

Linda D. Lee

Portland State University

Author Note

Linda D. Lee, College of Engineering, University of Alaska Anchorage.

This research is funded by the National Science Foundation grant no. 1758006 and was conducted at Portland State University. Special thanks to Steve Reichow and Bassam Haddad for direction and guidance for the research project and support throughout.

Correspondence concerning this paper should be addressed to Linda D. Lee, College of Engineering, University of Alaska Anchorage. Email: ldlee3@alaska.edu.

Abstract

Intercellular communication is vital for quick adjustments and maintenance for cell function and development. Gap junctions are membranes channel proteins that enable this direct communication between adjacent cells throughout the body. The compatibility of connexins (Cx), which make up a gap junction, determines whether a gap junction can form. Though many studies show which connexins are compatible, the molecular basis is not known (Bai & Wang, 2014). Through computational modeling, we identify the residues that energetically contribute most favorably at the docking interface of homotypic and heterotypic combinations of Cx43, Cx46, and Cx50 gap junctions. However, due to instability of the Cx43 homology model, calculations were only completed for gap junctions Cx46, Cx50 and Cx46-Cx50. The difference in energy profile of each respective model suggest a possible explanation for Cx46's docking promiscuity.

Keywords: connexin (Cx), compatibility, docking, interaction energy, homology modeling

Deciphering the Rules of Cell-to-Cell Coupling

by Molecular Modeling and Simulation

Introduction

Gap junctions are intercellular membrane channel proteins that facilitate direct communication by connecting the cytoplasm of two adjacent cells (Schadzek & Schlingmann et al., 2016). This form of cytoplasmic coupling allow for the exchange of ions and small molecules through the channel pore. Cell-to-cell communication is crucial for cell development and homeostasis throughout the body including the heart and the liver (Bai & Wang, 2014, Gong et al., 2013, Nakagawa et al., 2011, White et al. 1994). Thus, failure to form these channels prevent cells from proper coordination leading to an unstable and sick environment. As it follows, mutations affecting the formation and function of gap junctions have been linked to a number of diseases including hearing loss, Charcot-Marie-Tooth disease, central hypomyelination and cataracts (Bai, 2016, Gong et al., 2013, Nakagawa et al., 2011, Karademir et al., 2016, White et al., 1994).

Gap junctions are formed by the docking of two hemichannels located in the plasma membranes of two neighboring cells. Each hemichannel is formed by the oligomerization of six connexins. In humans, there are 21 genes encoding different connexins (Cx) isoforms (Gong et al., 2013, Jassim et al., 2016, Nakagawa et al., 2011, White et al. 1994). Though the 21 isoforms are not ubiquitously expressed throughout the body, expression of more than one connexin isoform is common in a given cell or tissue (White et al., 1994). The co-expression of multiple connexins within a gap junction diversifies the number of assemblies creating a complex network of unique channels with distinct permeabilities (Srinivas et al., 2017). Different assemblies include combinations of homomeric or heteromeric hemichannels where the hexamer is composed of only one connexin isoform or multiple

isoforms, respectively, and homotypic or heterotypic gap junctions where the two hemichannels are either identical or distinct, respectively. It is the interaction between these connexins that determine compatibility between hemichannels and allow the formation of a gap junction.

Docking happens in the extracellular region of the membrane proteins. A connexin has two extracellular loops (E1-E2) along with an N-terminus, C-terminus, and cytoplasmic loop in the intracellular region and four transmembrane domains (Bai & Wang, 2014). In 2009, the first high resolution crystal structure of a gap junction, connexin26 (Cx26), was determined by Maeda et al. Their structure revealed that E1 sits on the inside of the channel lining the pore while E2 lines the exterior (Maeda et al., 2009). Sequence alignment analyses reveal high sequence homology in the extracellular domains between different connexins indicating its significance to the proteins overall structure and function. (Bai, 2016, Jassim et al., 2016). E1 in particular shows high conservation suggesting an important role in channel formation (Nakagawa, 2011). E2, on the other hand, shows grouped conservation and through empirical studies, have been shown to be involved in docking specificity (Bai & Wang, 2014).

Based on the ability to form functional gap junction channels between homomeric hemichannels and based on sequence motifs in E2, ten well-studied connexins were divided into two groups, group I and group II (Karademir et al., 2016). Group I connexins comprise of Cx26, x30, Cx32, Cx46, and Cx50, while group II members include Cx30.3, Cx37, Cx40, Cx43, and Cx45 (Bai & Wang, 2014). In general, connexins within a group are compatible but not inter-group. These rules are not without exception, two particular connexins, Cx30 and Cx46, break this trend and exhibit an unusual behavior with mixed or conflicting inter-group data.

There are three connexin isoforms present in the eye lens, Cx43, Cx46, and Cx50 (Beyer & Berthoud, 2014). Although Cx43 belongs to group II and Cx46 and Cx50 belong to group I, Cx46 is

able to dock with Cx43. The different combinations of compatible and incompatible connexins make the eye lens a perfect model to observe possible differences in energetic properties involved in docking and formation of gap junctions. Thus, molecular dynamic (MD) simulations and energy calculations were conducted on different combinations of connexins in the eye lens to identify residues important in heterotypic coupling of gap junctions.

Materials and Methods

Construction of Cx43

The protein sequence for Cx43 was obtained from UnitProtKB (The UniProt Consortium, 2017) and used to create a homology model of homomeric-homotypic Cx43 via SWISS MODEL (Waterhouse et al., 2018). A high-resolution cryogenic electron microscopy (cryo-EM) structure of sheep Cx46, determined by the Reichow Lab, was used as a template for the model. The cryo-EM structure of Cx46 did not include the cytoplasmic loops or C-terminus of the connexins and was cut out in our final homology model of Cx43 using Visual Molecular Dynamics (VMD) v1.9.3 (Humphrey et al., 1996). Given its high sequence homology and our interest in the region, we aligned the proteins along the E1 domains. Nanoscale Molecular Dynamics (NAMD) was used to minimize the energy of the channel by steepest descent to avoid steric clashing between residues (Phillips et al., 2005). Each hemichannel of the gap junction model was incorporated into a 1-palmitoyl-2-oleoyl-sn-glycero-3-phosphocholine (POPC) membrane, hydrated, and ionized with 150 mM of KCl in the intracellular space and 150 mM of NaCl in the extracellular space.

Construction of Heterotypic Channels

The homology model of Cx43 was superimposed with a previously constructed gap junction models of Cx46 made by the Reichow Lab. Then opposing hemichannels of each structure were

deleted to create one heterotypic gap junction of Cx43-Cx46. The POPC membranes, water, and appropriate ions were added the same way as was done for the Cx43 homotypic model. This procedure was repeated with Cx50 to create a heterotypic model of Cx43-Cx50. For simplification, all models used were homomeric.

Simulation: Minimization and Equilibration

The energy of all three systems were minimized and simulations were run for 50 ns using NAMD. Each system was subject to three stages of minimization for 2 ns each. First the membrane was melted to relax the lipid tails. Then the protein was constrained to allow the membrane to fit around the protein. Last the protein backbone was constrained so that the protein sidechains could rearrange themselves into their most natural positions. After minimization, restraints were released and simulation was run for 20 ns to equilibrate the system then continued for 30 ns of production. The equilibration phase is to allow the protein backbone to reach a steady state before measurements are taken on the data. NAMD-Energy Plugin v.1.4, was used to calculate the total non-bonding interaction energies between all the atoms in the docking interface and then for each unique residue per connexin in one hemichannel against the whole docking interface of the opposing hemichannel. Non-bonding energies include energy from electrostatic and van der Waals interactions.

Results

Upon visual inspection, the Cx43 homology models were not stable. Holes formed in the extracellular regions allowing ions to freely flow in and out of the channel and the extracellular space. Thus calculations for the Cx43 models were forsaken and only the data from the Cx46 and Cx50 homotypic and heterotypic channels were collected.

We predicted that the interaction energy between hemichannels in the Cx43-Cx50 model would exhibit positive, or unfavorable, energy at the docking interface due to incompatibility. So, calculations were done between the whole docking interface of one hemichannel against the whole docking interface of the opposing hemichannel to verify the models were giving expected positive or negative energies depending on compatibility. Since we could not confidently calculate the interaction energy between Cx43 and Cx50 without a stable model, calculations were only carried out for Cx46 and Cx50 homotypic channels and the heterotypic Cx46-Cx50 channel. Interaction energies of the two docking interfaces are presented in Table 1.

Model	Total energy between docking interface v. opposing docking interface	Model	Sum of parsed energies of one docking residue v. whole opposing docking interface
Cx46-Cx46	-378 kcal/mol	Cx46-Cx46	-376 kcal/mol
Cx50-Cx50	-285 kcal/mol	Cx50-Cx50	-284 kcal/mol
Cx46-Cx50	-249 kcal/mol	Cx46*-Cx50	-251 kcal/mol
		Cx46-Cx50*	-251 kcal/mol

Table 1. Comparison of the sum of energies parsed by residue to the calculated total interaction energy at the docking interface. Calculations are absolute energies. Asterisks indicate which hemichannel single residue calculations were calculated from.

To look at the energy contribution from each residue to the overall docking interaction, one residue per connexin in one hemichannel was selected against the whole docking interface of the opposing hemichannel for calculations. Four sets of data were produced, total interaction energy between: residues from Cx46 against the whole interface of Cx46 hemichannel, residues from Cx50 against the whole interface of the Cx50 hemichannel, residues of Cx46 against the whole interface of Cx50 hemichannel, and residues of Cx50 against the whole interface of Cx46 hemichannel. The sum of the energies for each residue in one channel were nearly equivalent to the interaction energy calculations between the whole docking interface against the opposing docking interface (Table 1).

For comparison, the calculations were normalized by converting the average total energy of each residue into their percent contribution to the total interaction energy at the docking interface. Figure 1a. shows the percent contributions for each residue in Cx50 in a homotypic (pink) and heterotypic (purple) system. Figure 1b. shows the percent contributions for each residue in Cx46 in a homotypic (light blue) and heterotypic (dark blue) system.

a.

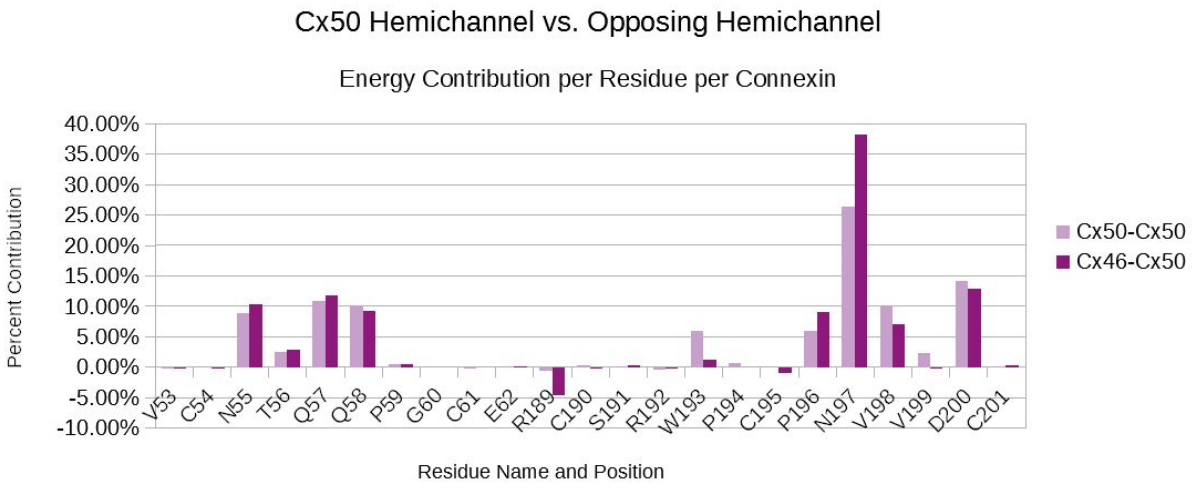

b.

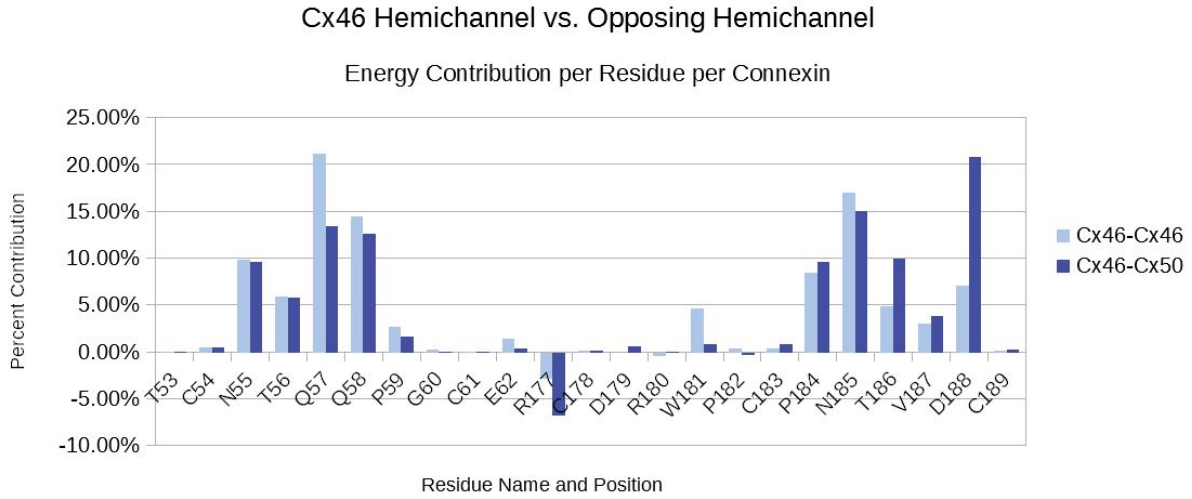

Figure 1. Percent contribution by residue to the total interaction energy at the docking interface. This graph represents the contribution of the same one residue in each connexin in one hemichannel against the whole docking interface of the opposite hemichannel. The asterisk indicates which hemichannel the single residues were calculated from.

(a) Comparison of Cx50 homotypic versus heterotypic coupling. (b) Comparison of Cx46 homotypic versus heterotypic coupling.

	Percent Contribution of E1	Percent Contribution of E2
Cx50-Cx50	34%	66%
Cx46-Cx50*	35%	65%
Cx46-Cx46	57%	43%
Cx46*-Cx50	45%	56%

Table 2. Percent contribution of extracellular domains to the total interaction energy at the docking interface. Asterisks indicate which hemichannel single residue calculations were calculated from.

When the energies are summed up according to extracellular domains, the contributions of each domain show similar distributions in Cx50 homotypic and heterotypic channels (Table 2). The prominent contributor in homotypic and heterotypic Cx50 models was N197. However, in Cx46, the percent contributions of E1 and E2 were flipped (see Table 2). The top contributing residue also shifted from Q57 in E1 for homotypic Cx46 to D188 in E2 of the heterotypic model, both contributing 21% to the total interaction energy (see Figure 2b).

Discussion

The failure to produce a stable homology model of Cx43 led us to abandon cross-group analysis of heterotypic coupling. The compatible hemichannels of homotypic Cx43 pulling apart suggests that the structure of a group I gap junction is not adequate to use as a template for Group II gap junctions. More knowledge is needed on the structure of group II connexins before convincing measurements and conclusions can be made. However, the energy profiles rendered from Cx46 and Cx50 homotypic and heterotypic coupling may provide a possible explanation for Cx46's ability to intermingle between groups.

The residues in Cx50 homotypic and heterotypic channels have similar energetic profiles with one noticeable difference, N197 in the transition from homotypic to heterotypic docking. N197 contributes 27% of the total non-bonding energy in homotypic docking of Cx50. It is also a hydrogen bond forming residue and mutations of this residue is linked to cataract formation in the lens (S. Reichow, personal communication, August 20, 2018, Nakagawa et al., 2011, Schadzek & Schlingmann et al., 2016). Though the significance of N197 is not novel, the jump to 38% non-bonding energy contribution in heterotypic docking further supports Cx50's dependence on N197.

In Cx46 there is a shift in the prominent residue from Q57 in the non-bonding energy contribution in homotypic docking to D188 in heterotypic docking. This change in energy contribution shifts the majority contribution from E1 in homotypic docking to E2 in heterotypic docking. This raises a new hypothesis that Cx46 is more flexible and able to shift or change to make itself more compatible to its binding partner, pointing to a potential explanation for Cx46's more friendly nature.

Conclusion and Future Directions

In conclusion, we found that using a group I connexin as a template is not sufficient to create a stable theoretical model of group II connexins. Also, the difference in the energy profiles between extracellular domains from homotypic to heterotypic forms in the compatible lens connexins, Cx46 and Cx50, reveal a more adaptive nature of Cx46 as opposed to the rigid nature of Cx50. To further support this hypothesis, a group II connexin need be elucidated in order to more accurately model and simulate cross-group interactions. Additional future work may be to continue energy profiling for the other group I connexins.

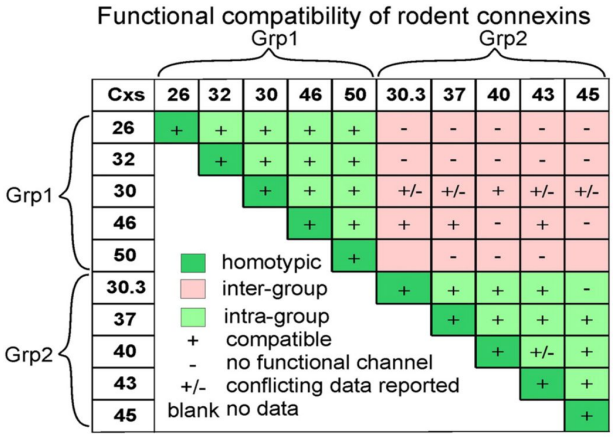

Figure 2. Heterotypic compatibility of ten selected connexins. Figure taken from Bai, D., & Wang, A. H. (2014). Extracellular domains play different roles in gap junction formation and docking compatibility. *The Biochemical Journal*, *458*(1), 1–10.

According to the compatibility chart (Figure 2), similar to Cx50, Cx26 and Cx32 are more conservative while Cx30 is more promiscuous like Cx46. If these connexins display the same sort of pattern between homotypic and heterotypic coupling, it could shed light on the validity of the claim that promiscuity is due to adaptability and may be worthwhile to investigate deeper into the underlying mechanism.

References

Bai, D. (2016). Structural analysis of key gap junction domains – Lessons from genome data and disease-linked mutants. Seminars in Cell & Developmental Biology, 50, 74–82. https://doi.org/10.1016/j.semcdb.2015.11.015

Bai, D., & Wang, A. H. (2014). Extracellular domains play different roles in gap junction formation and docking compatibility. *The Biochemical Journal*, *458*(1), 1–10. https://doi.org/10.1042/BJ20131162

Beyer, E. C., & Berthoud, V. M. (2014). Connexin hemichannels in the lens. *Frontiers in Physiology*, *5*, 20. https://doi.org/10.3389/fphys.2014.00020

Gong, X.-Q., Nakagawa, S., Tsukihara, T., & Bai, D. (2013). A mechanism of gap junction docking revealed by functional rescue of a human-disease-linked connexin mutant. Journal of Cell Science, 126(14), 3113–3120. https://doi.org/10.1242/jcs.123430

Humphrey, W., Dalke, A. and Schulten, K., `VMD – Visual Molecular Dynamics', J. Molec. Graphics 1996, 14.1, 33-38.

Jassim, A., Aoyama, H., Ye, W. G., Chen, H., & Bai, D. (2016). Engineered Cx40 variants increased docking and function of heterotypic Cx40/Cx43 gap junction channels. Journal of Molecular and Cellular Cardiology, 90, 11–20. https://doi.org/10.1016/j.yjmcc.2015.11.026

Karademir, L. B., Aoyama, H., Yue, B., Chen, H., & Bai, D. (2016). Engineered Cx26 variants established functional heterotypic Cx26/Cx43 and Cx26/Cx40 gap junction channels. The Biochemical Journal, 473(10), 1391–1403. https://doi.org/10.1042/BCJ20160200

Nakagawa, S., Gong, X.-Q., Maeda, S., Dong, Y., Misumi, Y., Tsukihara, T., & Bai, D. (2011). Asparagine 175 of connexin32 is a critical residue for docking and forming functional

heterotypic gap junction channels with connexin26. The Journal of Biological Chemistry, 286(22), 19672–19681. https://doi.org/10.1074/jbc.M110.204958

Phillips, J. C., Braun, R., Wang, W., Gumbart, J., Tajkhorshid, E., Villa, E., Chipot, C., Skeel, R. D., Kale, L., and Schulten, K. Scalable molecular dynamics with NAMD. *Journal of Computational Chemistry*, 26:1781-1802, 2005.

Schadzek, P., Schlingmann, B., Schaarschmidt, F., Lindner, J., Koval, M., Heisterkamp, A., … Ngezahayo, A. (2016). The cataract related mutation N188T in human connexin46 (hCx46) revealed a critical role for residue N188 in the docking process of gap junction channels. Biochimica Et Biophysica Acta, 1858(1), 57–66. https://doi.org/10.1016/j.bbamem.2015.10.001

Srinivas, M., Verselis, V. K., & White, T. W. (2018). Human diseases associated with connexin mutations. *Biochimica et Biophysica Acta (BBA) - Biomembranes*, *1860*(1), 192–201. https://doi.org/10.1016/j.bbamem.2017.04.024

The UniProt Consortium. (2017) UniProt: the universal protein knowledgebase. Nucleic Acids Res, 45, D158-D169.

Waterhouse, A., Bertoni, M., Bienert, S., Studer, G., Tauriello, G., Gumienny, R., Heer, F.T., de Beer, T.A.P., Rempfer, C., Bordoli, L., Lepore, R., Schwede, T. SWISS-MODEL: homology modelling of protein structures and complexes. Nucleic Acids Res. 46(W1), W296-W303 (2018).